Hindawi
Mathematical Problems in Engineering
Volume 2020, Article ID 9584854, 12 pages
https://doi.org/10.1155/2020/9584854

Research Article

The Shape Effect of Gold Nanoparticles on Squeezing Nanofluid Flow and Heat Transfer between Parallel Plates

Umair Rashid,[1] Thabet Abdeljawad,[2,3,4] Haiyi Liang,[1,5] Azhar Iqbal,[6] Muhammad Abbas,[7] and Mohd. Junaid Siddiqui[6]

[1]*CAS Key Laboratory of Mechanical Behavior and Design of Materials, Department of Modern Mechanics, University of Science and Technology of China, Hefei, Anhui 230026, China*
[2]*Department of Mathematics and General Sciences, Prince Sultan University, Riyadh 11586, Saudi Arabia*
[3]*Department of Medical Research, China Medical University, Taichung 40402, Taiwan*
[4]*Department of Computer Science and Information Engineering, Asia University, Taichung 40402, Taiwan*
[5]*IAT-Chungu Joint Laboratory for Additive Manufacturing, Anhui Chungu 3D Printing Institute of Intelligent Equipment and Industrial Technology, Wuhu, Anhui 241200, China*
[6]*Mathematics and Natural Sciences, Prince Mohammad Bin Fahd University, Al Khobar 31952, Saudi Arabia*
[7]*Department of Mathematics, University of Sargodha, Sargodha 40100, Pakistan*

Correspondence should be addressed to Thabet Abdeljawad; tabdeljawad@psu.edu.sa and Haiyi Liang; hyliang@ustc.edu.cn

Received 1 July 2020; Accepted 5 August 2020; Published 2 September 2020

Academic Editor: Marin Marin

The focus of the present paper is to analyze the shape effect of gold (Au) nanoparticles on squeezing nanofluid flow and heat transfer between parallel plates. The different shapes of nanoparticles, namely, column, sphere, hexahedron, tetrahedron, and lamina, have been examined using water as base fluid. The governing partial differential equations (PDEs) are transformed into ordinary differential equations (ODEs) by suitable transformations. As a result, nonlinear boundary value ordinary differential equations are tackled analytically using the homotopy analysis method (HAM) and convergence of the series solution is ensured. The effects of various parameters such as solid volume fraction, thermal radiation, Reynolds number, magnetic field, Eckert number, suction parameter, and shape factor on velocity and temperature profiles are plotted in graphical form. For various values of involved parameters, Nusselt number is analyzed in graphical form. The obtained results demonstrate that the rate of heat transfer is maximum for lamina shape nanoparticles and the sphere shape of nanoparticles has performed a considerable role in temperature distribution as compared to other shapes of nanoparticles.

1. Introduction

Nanotechnology has recently emerged and has become a worldwide revolution to obtain exceptional qualities and features over the last few decades. It developed at such a fast pace and is still going through a revolutionary phase. Nanotechnology is coming together to play a crucial and commercial role in our future world. Gold nanoparticles are one of the utmost stable metal nanoparticles and their current fascinating features include assembly of several types in material science, individual nanoparticles behaviors, magnetic, nanocytotoxic, optical properties, size-related electronic, significant catalysis, and biological applications. Gold nanoparticles have attracted research attention due to their properties and various potential applications. This progression would go to the later generation of nanotechnology that requires products of gold nanoparticles with precise shape, controlled size, large production facilities, and pureness. Gold nanoparticles are widely used as preferred materials in numerous fields because of their unique optical and physical properties, that is, surface plasmon oscillation for labeling, sensing, and imaging. Recently, significant developments have been made in biomedical fields with superior biocompatibility in therapeutics and treatment of various diseases. Gold nanoparticles can be prepared and conjugate

with numerous functionalizing agents such as dendrimers, ligands, surfactants, RNA, DNA, peptides, polymers, oligonucleotides, drugs, and proteins [1].

Squeezing nanofluid flow with the effect of thermal radiation and magnetohydrodynamics (MHD) has important uses in the development of the real world. It has gained the consideration of researchers due to its extensive usages. Squeezing flow has increasing usages in several areas, particularly in the food industry and chemical engineering. The undertakings and properties of the squeezing flow of nanofluid for industrial usages such as electronic, transportation, biomechanics, foods, and nuclear reactor have been explained in many publications in the open literature. There are various examples concerning squeezing flow but the most significant ones are injection, compression, and polymer preparation.

The squeezing flow of nanofluid has gained significant consideration due to the valuable verities of applications in the physical and biophysical fields [2]. Hayat et al. [3] discussed the MHD in squeezing flow by using two disks. Dib et al. [4] examined the analytical solution of squeezing nanofluid flow. Duwairi et al. [5] addressed the heat transfer on the viscous squeezed flow between parallel plates. Domairry and Hatami [6] examined the time-dependent squeezing of nanofluid flow between two surfaces by applying differential transformation techniques. Sheikholeslami and Ganji [7] studied the heat transfer in squeezed nanofluid flow based on homotopy perturbation method. The thermal radiation effect in two-dimensional and time-dependent squeezing flow was investigated using homotopy analysis method by Khan et al. [8]. Sheikholeslami et al. [9] presented the effect of MHD on squeezing nanofluid flow in a rotating system. Gupta and Saha Ray [10] investigated the unsteady squeezing nanofluid flow between two parallel plates by using the Chebyshev wavelet expansion. The effects of MHD on alumina-kerosene nanofluid and heat transfer within two horizontal plates were examined by Mahmood and Kandelousi [11].

In the fields of engineering and science, there are various mathematical problems to find but the exact solution is almost complicated. Homotopy analysis method (HAM) is a well-known and critical method for solving mathematics-related problems. The main advantage of the homotopy analysis method is finding the approximate solution to the nonlinear differential equation without linearization and discretization. Earlier time in 1992, Liao [12–16] introduced this technique to find out the analytical results of nonlinear problems. The author concluded that homotopy analysis method (HAM) quickly converges to an approximate solution. The homotopy analysis method gives us a series of solutions. The approximate solution by homotopy analysis method is quite perfect since it contained all the physical parameters involved in a problem. Due to the effectiveness and quick convergence of the solution, various researchers, namely, Rashidi et al. [17, 18] and Abbasbandy and Shirzadi [19, 20], used homotopy analysis method (HAM) to find the solutions of highly nonlinear and coupled equations. Hussain et al. [21] presented the bioconvection model for squeezing flow using homotopy analysis method with the effect of thermal radiation heat generation/absorption.

Heat transfer can be increased by using several methodologies and techniques such as increasing the heat transfer coefficient or heat transfer surface which allows for a higher heat transfer rate in small volume fraction. Cooling is a major technical challenge faced by increasing numbers of industries involving microelectronics, transportation, manufacturing, and solid-state lighting. So, there is an essential requirement for innovative coolant with a better achievement that would be employed for enhanced properties [22]. Recently, nanotechnology has contributed to improving the new and innovative class of heat transfer nanofluid. Base fluids are embedded with nanosize materials to obtain nanofluids (nanofibers, nanoparticles, nanotubes, nanorods, nanowires, droplet, or nanosheet) [23]. Significantly, nanofluids have the ability to enhance heat transfer rate in several areas like nuclear reactors, solar power plants, transportation industry (trucks, automobiles, and airplanes), electronics and instrumentation, biomedical applications, microelectromechanical system, and industrial cooling usages (cancer therapeutics, cryopreservation, and nanodrug delivery) [24]. There are several studies to show the applications of nanofluid heat transfer. Kristiawan et al. [25] studied the convective heat transfer in a horizontal circular tube using TiO_2-water nanofluid. Turkyilmazoglue and Pop discussed the heat and mass transfer of convection flow of nanofluids containing nanoparticles of Ag, Cu, TiO_2, Al_2O_3, and CuO [26]. Sheikholeslami and Ganji [7] presented the analytical results of heat transfer in water-Cu nanofluid. Qiang and Yimin [27] investigated the experimental studies of convective heat transfer in water-Cu nanofluid. Elgazery [28] examined the studies of Ag-Cu-Al_2O_3-TiO_2-water nanofluid over a vertical permeable stretching surface with a nonuniform heat source/sink. Rea et al. [29] studied the viscous pressure and convective heat transfer in a vertical heated tube of Al_2O_3-ZrO_2-water nanofluids. Salman et al. [30] discussed by using a numerical technique the concept of affecting convective heat transfer of nanofluid in microtube using different categories of nanoparticles such as Al_2O_3, Cuo, SiO_2, and ZnO. Sheikholeslami et al. [31, 32] studied hybrid nanofluid for heat transfer expansion. Hassan et al. [33] discussed convective heat transfer in Ag-Cu hybrid nanofluid flow. Bhatti et al. [34] examined numerically hall current and heat transfer effects on the sinusoidal motion of solid particles. Furthermore, many researchers did work on heat transfer and thermal radiation; see [35–39].

In light of the above literature study, it has been observed that Cu, Ag, Al_2O_3, SiO_2, Cuo, and ZnO are mostly used to find the heat transfer. The gold (Au) was rarely used to find the heat transfer rate due to mixed convection [40]. The shape of nanoparticles is very significant in the enhancement of heat transfer. It is necessary to find the heat transfer rate in nanofluid under the exact shapes of nanoparticles [41]. From the literature survey, it is observed that no effort has been made on gold (Au) nanoparticles shape effect on squeezing flow. The basic purpose of the present study is to analyze the shape effect of gold (Au) nanoparticles on squeezing nanofluid flow and heat transfer. Various types of nanoparticles are under deliberation: column, sphere, hexahedron, tetrahedron, and lamina. The effects of various

physical parameters on velocity and temperature distributions are analyzed through plotted graphs.

2. Problem Description

Consider heat transfer in the incompressible, two-dimensional, laminar, and stable squeezing nanofluid between two horizontal plates at $y = 0$ and $y = h$. The lower plate is fixed by two forces which are equal and opposite. Both the plates are separated by distance h. A uniform B magnetic field is applied along y-axis. Moreover, the effect of nonlinear thermal radiation is also considered. The thermophysical properties of gold nanoparticles and water are presented in Table 1. The values of nanoparticles shapes-related parameters are presented in Table 2. The partial governing equations of the problem are modeled as [42]

$$\frac{\partial u}{\partial x} + \frac{\partial v}{\partial y} = 0, \tag{1}$$

$$u\frac{\partial u}{\partial x} + v\frac{\partial u}{\partial y} = -\frac{1}{\rho_{n_f}}\frac{\partial p}{\partial x} + \frac{\mu_{n_f}}{\rho_{n_f}}\left(\frac{\partial^2 u}{\partial x^2} + \frac{\partial^2 u}{\partial y^2}\right) - \frac{\sigma_{n_f} B^2 u}{\rho_{n_f}}, \tag{2}$$

$$u\frac{\partial v}{\partial y} = -\frac{1}{\rho_{n_f}}\frac{\partial p}{\partial y} + \frac{\mu_{n_f}}{\rho_{n_f}}\left(\frac{\partial^2 u}{\partial x^2} + \frac{\partial^2 u}{\partial y^2}\right), \tag{3}$$

$$\begin{aligned} u\frac{\partial T}{\partial x} + v\frac{\partial T}{\partial y} &= \frac{k_{n_f}}{(\rho Cp)_{nf}}\left(\frac{\partial^2 T}{\partial x^2} + \frac{\partial^2 T}{\partial y^2}\right) + \frac{\mu_{n_f}}{(\rho Cp)_{nf}} \\ &\cdot \left\{2\left[\left(\frac{\partial u}{\partial x}\right)^2 + \left(\frac{\partial v}{\partial y}\right)^2\right] + \left(\frac{\partial v}{\partial x}\right)^2\right\} \\ &+ \frac{16\sigma^*}{3(\rho Cp)_{nf} K^*}\frac{\partial^2 T}{\partial y^2}. \end{aligned} \tag{4}$$

The reverent boundary value conditions are

$$\begin{aligned} f = 0, f' = 1, \theta = 1, \quad \text{at } \eta = 0, \\ f = \frac{v_0}{ah}, f' = 0, \theta = 0, \quad \text{at } \eta = 1. \end{aligned} \tag{5}$$

The following similarity variables are induced to nondimensionalize governing equations (1)–(4):

$$\begin{aligned} u &= axf'(\eta), \\ v &= -ahf(\eta), \\ \eta &= \frac{y}{h}, \\ \theta(\eta) &= \frac{T - T_1}{T_2 - T_1}. \end{aligned} \tag{6}$$

Equation (1) is identically satisfied. Eliminating the pressure and by using equation (6) into equations (2), (3), and (4), one has the following nonlinear coupled boundary value problems:

Table 1: Thermophysical properties of gold (Au) and pure water as [40, 43].

Physical properties	Gold (Au)	Pure water
ρ (kg/m^3)	19300	998.3
Cp (J/kg·K)	129	4182
k (W/m·K)	318	0.60

Table 2: The values of nanoparticles shapes-related parameters as [44].

Shapes	Column	Sphere	Hexahedron	Tetrahedron	Lamina
ϕ	0.4710	1	0.8060	0.7387	0.1857
m	6.3698	3	3.7221	4.0613	16.1576

$$f'''' - R\frac{A_1}{A_2}\left(f'f'' - ff'''\right) - \frac{1}{A_2}Mf'' = 0, \tag{7}$$

$$(1 + \mathrm{Rd})\theta'' + \mathrm{Pr}\left(\frac{A_3}{A_4}Rf\theta' + 4\frac{A_2}{A_4}\mathrm{Ec}f'^2\right) = 0, \tag{8}$$

$$\begin{aligned} f(0) &= 0, \\ f'(0) &= 1, \\ f(1) &= A, \\ f'(1) &= 0, \\ \theta(0) &= 1, \\ \theta(\infty) &= 0. \end{aligned} \tag{9}$$

The dimensionless quantities are

$$\begin{aligned} A &= \frac{v_0}{ah}, \\ R &= \frac{ah^2}{v_f}, \\ \mathrm{Pr} &= \frac{\mu_f (\rho Cp)_f}{\rho_f k_f}, \\ \mathrm{Ec} &= \frac{\rho_f a^2 h^2}{(\rho Cp)_f (T_w - T_\infty)}, \\ M &= \frac{\sigma_{n_f} B^2 h^2}{v_f \rho_f}, \\ \mathrm{Rd} &= \frac{16\sigma^* T_\infty^3}{3k_{n_f} k^*}. \end{aligned} \tag{10}$$

Here, A, Pr, M, R, Ec, and Rd represent the suction parameter, Prandtl number, magnetic parameter, Reynolds number, Eckert number, and thermal radiation parameter, respectively. One has

$$A_1 = \frac{\rho_{n_f}}{\rho_f},$$
$$A_2 = \frac{\mu_{n_f}}{\mu_f},$$
$$A_3 = \frac{(\rho Cp)_{nf}}{(\rho Cp)_f},$$
$$A_4 = \frac{k_{n_f}}{k_f}. \tag{11}$$

Here, A_1, A_2, A_3, and A_4 represent the ratio of density, viscosity, heat capacitances, and thermal conductivity, respectively.

In this study, we consider

$$\frac{\rho_{n_f}}{\rho_f} = (1-\phi) + \frac{\rho_s}{\rho_f}\phi,$$
$$\frac{\mu_{n_f}}{\mu_f} = \frac{1}{(1-\phi)^{2.5}},$$
$$\frac{(\rho Cp)_{nf}}{(\rho Cp)_f} = (1-\phi) + \frac{(\rho Cp)_s}{(\rho Cp)_f}\phi,$$
$$\frac{k_{n_f}}{k_f} = \frac{\left[k_s + (m-1)k_f\right] - (m-1)\phi\left(k_f - k_s\right)}{\left[k_S + (m-1)k_f\right] + \phi\left(k_f - k_s\right)}, \tag{12}$$

where k_f, μ_f, ρ_f, and $(\rho Cp)_f$ represent thermal conductivity, dynamic viscosity, density, and specific heat of the fluid, respectively, whereas k_s, μ_s, ρ_s, and $(\rho Cp)_s$ denote the thermal conductivity, dynamic viscosity, density, and specific heat of the solid, respectively. m and ϕ are the shape factor and volume fraction of nanoparticles, respectively.

The physical quantity of Nu (Nusselt number) is defined as

$$\mathrm{Nu} = \left|A_4\theta'(0)\right|. \tag{13}$$

3. Solution by HAM

The auxiliary linear operators are selected as follows:

$$\mathscr{L}_f(f) = \frac{\mathrm{d}^4 f}{\mathrm{d}\eta^4},$$
$$\mathscr{L}_\theta(\theta)\frac{\mathrm{d}^2\theta}{\mathrm{d}\eta^2}. \tag{14}$$

These auxiliary operators satisfy the following properties:

$$\mathscr{L}_f\left[C_1\frac{\eta^3}{6} + C_2\frac{\eta^2}{2} + C_3\eta + C_4\right] = 0,$$
$$\mathscr{L}_\theta\left[C_5 e^{\eta} + C_6 e^{-\eta}\right] = 0. \tag{15}$$

The initial guesses are chosen as

$$f_0(\eta) = (1-2A)\eta^3 + (3A-2)\eta^2 + \eta,$$
$$\theta_0(\eta) = 1 - \eta. \tag{16}$$

3.1. Zeroth-Order Deformation. The corresponding zeroth deformation problem is defined as follows:

$$(1-q)\mathscr{L}_f\left[\widehat{f}(\eta,q) - f_0(\eta)\right] = q\hbar_f\mathscr{N}_f\left[\widehat{f}(\eta,q), \widehat{\theta}_0(\eta,q)\right],$$
$$\widehat{f}(0,q) = 0,$$
$$\widehat{f}'(0,q) = 1,$$
$$\widehat{f}(1,q) = A,$$
$$\widehat{f}'(1,q) = 0,$$
$$(1-q)\mathscr{L}_\theta\left[\widehat{\theta}(\eta,q) - \theta_0(\eta)\right] = q\hbar_\theta\mathscr{N}_\theta\left[\widehat{\theta}_0(\eta,q), \widehat{f}(\eta,q)\right],$$
$$\widehat{\theta}(0,q) = 1,$$
$$\widehat{\theta}(1,q) = 0, \tag{17}$$

in which $q\epsilon[0,1]$ is called an embedding parameter and $\hbar_f \neq 0$ and $\hbar_\theta \neq 0$ are the convergence control parameters such that $\widehat{f}(\eta,0) = f_0(\eta), \widehat{\theta}(\eta,0) = \theta_0(\eta)$ and $\widehat{f}(\eta,1) = f(\eta), \widehat{\theta}(\eta,1) = \theta(\eta)$; it means that when q varies from 0 to 1, $\widehat{f}(\eta,q)$ varies from initial guess $f_0(\eta)$ to the final solution $f(\eta)$ and $\widehat{\theta}(\eta,q)$ varies from initial guesses $\theta_0(\eta)$ to $\theta(\eta)$.

The nonlinear operators $\mathscr{N}_f$ and $\mathscr{N}_\theta$ are given by

$$N_f[\widehat{f}(\eta,q), \widehat{\theta}(\eta,q)] = \frac{\partial^4\widehat{f}(\eta,q)}{\partial\eta^4} - \frac{A_1}{A_2}R\left(\frac{\partial\widehat{f}(\eta,q)}{\partial\eta}\frac{\partial^2\widehat{f}(\eta,q)}{\partial\eta^2} - \widehat{f}(\eta,q)\frac{\partial^3\widehat{f}(\eta,q)}{\partial\eta^3}\right) - \frac{1}{A_2}M\frac{\partial^2\widehat{f}(\eta,q)}{\partial\eta^2} = 0,$$
$$N_\theta[\widehat{\theta}(\eta,q), \widehat{f}(\eta,q)] = (1+R_d)\frac{\partial^2\widehat{\theta}(\eta,q)}{\partial\eta^2} + \mathrm{Pr}\left(\frac{A_3}{A_4}R\widehat{f}(\eta,q)\frac{\partial\widehat{\theta}(\eta,q)}{\partial\eta} + 4\frac{A_2}{A_4}\mathrm{Ec}\frac{\partial^2\widehat{f}(\eta,q)}{\partial\eta^2}\right) = 0. \tag{18}$$

Expanding $\widehat{f}(\eta, q)$ and $\widehat{\theta}(\eta, q)$ with respect to q Maclaurin's series and $q = 0$, we obtain

$$f(\eta, q) = f_0(\eta) + \sum_{m=1}^{\infty} f_m(\eta) q^m,$$
$$\theta(\eta, q) = \theta_0(\eta) + \sum_{m=1}^{\infty} \theta_m(\eta) q^m, \tag{19}$$

where $f_m(\eta) = (1/m!)\left((\partial^m f(\eta, q))/(\partial \eta^m)\right)|_{q=0}$ and $\theta_m(\eta) = (1/m!)\left((\partial^m \theta(\eta, q))/(\partial \eta^m)\right)|_{q=0}$.

3.2. Higher-Order Deformation Problem. The higher-order problems are as follows:

$$\mathscr{L}_f\left[f_m(\eta) - \chi_m f_{m-1}(\eta)\right] = \hbar_f \mathscr{R}_f^m\left(f_{m-1}(\eta), \theta_{m-1}(\eta)\right),$$
$$f_m(0) = 0,$$
$$f_m'(0) = 0,$$
$$f_m'(1) = 0,$$
$$f_m'(1) = 0,$$
$$\mathscr{L}L_f\left[\theta_m(\eta) - \chi_m \theta_{m-1}(\eta)\right] = \hbar_\theta \mathscr{R}_\theta^m\left(\theta_{m-1}(\eta), f_{m-1}(\eta)\right),$$
$$\theta_m(0) = 0,$$
$$\theta_m(1) = 0, \tag{20}$$

where

$$\chi_m = \begin{cases} 0, & \text{when } m \le 1, \\ 1, & m > 1, \end{cases}$$

$$\mathscr{R}_f^m f_m(\eta) = f_{m-1}''(\eta) - \frac{A_1}{A_2} R \cdot \left(\sum_{z=0}^{m-1} f_z' f_{m-1-z}'' - \sum_{z=0}^{m-1} f_z f_{m-1-z}''\right) - M f_{m-1}''(\eta),$$

$$\mathscr{R}_f^m \theta_m(\eta) = (1 + R_d)\theta_{m-1}'' + \Pr \frac{A_3}{A_4} R \cdot \left(\sum_{z=0}^{m-1} f_z \theta_{m-1-z}' + 4 \frac{A_2}{A_4} \mathrm{Ec} \sum_{z=0}^{m-1} f_z'' f_{m-1-z}''\right). \tag{21}$$

The m^{th}-order solutions are

$$f_m(\eta) = f_m^* + C_1 \frac{\eta^3}{6} + C_2 \frac{\eta^2}{2} + C_3 \eta + C_4, \tag{22}$$

$$\theta_m(\eta) = \theta_m^* + C_5 e^{\eta} + C_6 e^{-\eta}, \tag{23}$$

where $C_z^m (z = 1 - 6)$ are constants to be determined by using the boundary conditions.

3.3. Convergence of Series Solutions. Zeroth- and higher-order deformation problems are given in equations (7) and (8), which clearly show that the series solutions contain nonzero auxiliary parameters $\hbar_f$ and $\hbar_\theta$. The convergence of the solutions is checked through plotting $\hbar$-curves $\hbar_f$ and $\hbar_\theta$ as displayed in Figures 1 and 2. It is evident that the series solutions (22) and (23) converge when $-1.8 \ge \hbar_f \le -0.2$ and $-1.8 \ge \hbar_\theta \le -0.2$.

4. Results and Discussion

The physical insight of the problem is discussed in this present portion. The schematic model of squeezing nanofluid is shown in Figure 3. The dynamics of heat transfer in the squeezing nanofluid fluid flow are described under the variation of dimensionless solid volume fraction, thermal radiation, Reynolds number, magnetic field, Eckert number, suction parameter, and shape factor. The analysis is carried out using the following range of parameters $0.1 \ge \phi \le 0.2$, $0.5 \ge A \le 1.0, 0.5 \ge M \le 4.0, 0.5 \ge R \le 1.0, 0.01 \ge \mathrm{Ec} \le 0.9$, and $0.5 \ge \mathrm{Rd} \le 2.0$. It is evident from Figures 4–7 that nanoparticles which participate in heat transfer are lamina > column > tetrahedron > hexahedron > sphere.

ϕ is a very important parameter for squeeze flow of nanofluid. From Figure 8, it is noted that the impact of ϕ on primary velocity seemed ineffective. It is also observed that the primary velocity is increased with increase of R as displayed in Figure 9. It is because that the inertia with the viscous ratio is dominant. From Figure 10, it is observed that the effect of M on the primary velocity is decreased due to the Lorentz force produced by M. The Lorentz force acts against the motion of squeeze flow of nanofluid. The variation of A on the dimensionless primary velocity is shown in Figure 11. From Figure 11, it can be seen that the primary velocity is intensifying with the increase of A; physically, the wall shear stress increases with the increase of A.

The secondary velocity decreases in the half of the region as shown in Figure 12. In Figures 13 and 14, it is distinguished that secondary velocity changed in half of the region (the region above the central line between the plates). It happened due to the constraint of law of conservation of mass. The variation of A is plotted in Figure 15; secondary velocity is also increased with the increase of A.

The shape effects of nanoparticles on dimensionless temperatures profiles are shown in Figure 16. It is noted from Figure 16 that sphere > hexahedron > tetrahedron > column > lamina. It is also observed that lamina nanoparticles have minimum temperature because of maximum viscosity while sphere shape nanoparticles have maximum temperature because of minimum viscosity. From Figure 17, it is observed that the temperature profile has a direct relation with ϕ; the reason is that increasing the volume fraction causes enhanced thermal conductivity of the nanofluid which turns to increase the boundary layer thickness. From Figure 17, it is also observed that the sphere shape nanoparticles show a prominent role in temperature distribution. Figure 18 depicts the influence of R on the dimensionless temperature profile; with increasing R, the dimensionless temperature profile decreases because of decreasing the thermal layer thickness. Figure 18 showed

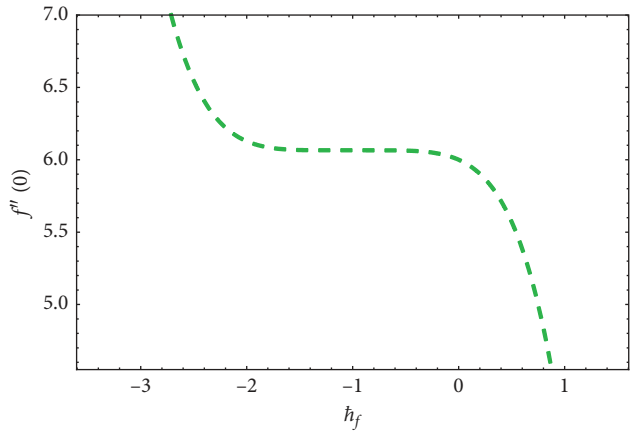

Figure 1: The $\hbar_f$–curve for $f''(0)$.

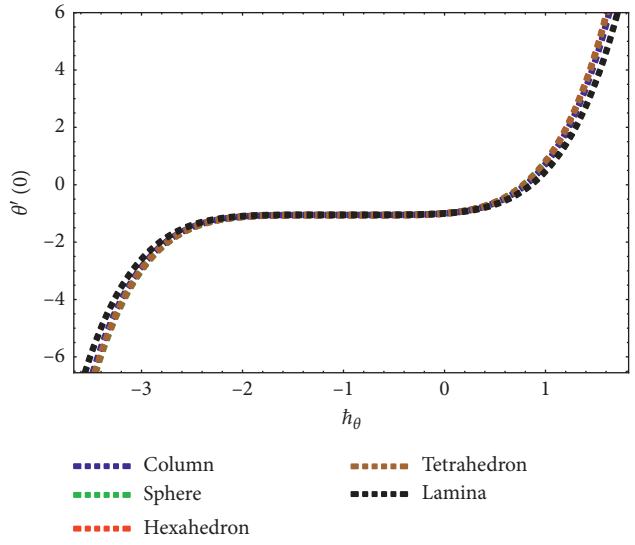

Figure 2: The $\hbar_\theta$–curve for $\theta'(0)$.

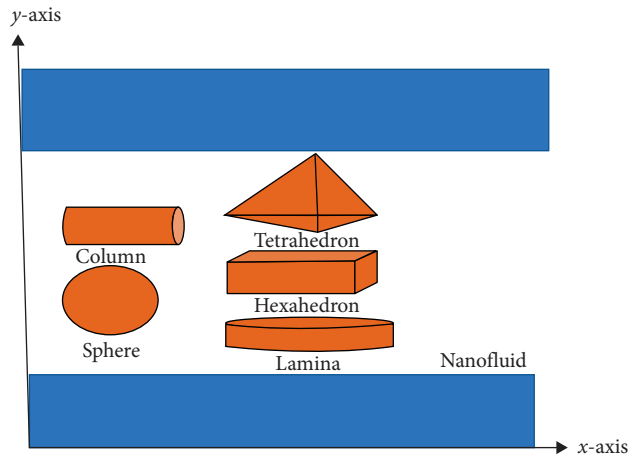

Figure 3: Schematic model of squeezing nanofluid.

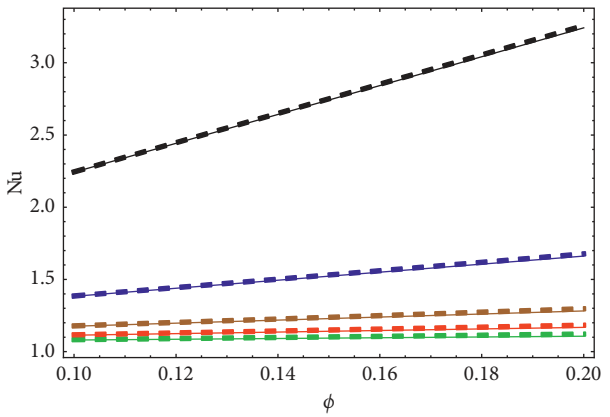

Figure 4: Nu for values of R and M, A, Rd = 0.5 and Ec = 0.3. Blue: column. Green: sphere. Red: hexahedron. Brown: tetrahedron. Black: lamina. $R = 0.5$ solid line; $R = 1.0$ dash line.

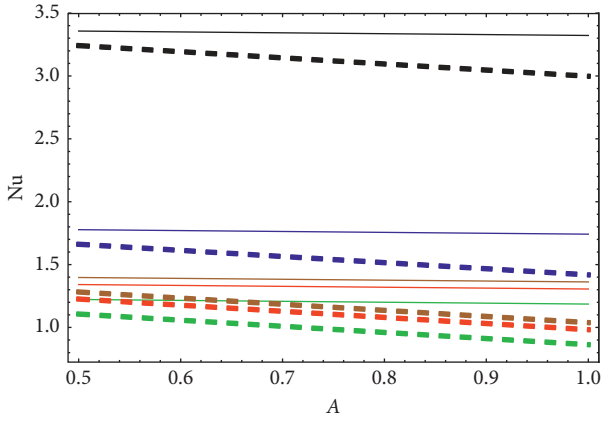

Figure 5: Nu for values of Ec and M, R, Rd = 0.5 and $\phi = 0.2$. Blue: column. Green: sphere. Red: hexahedron. Brown: tetrahedron. Black: lamina. Ec = 0.01 solid line; Ec = 0.03 dash line.

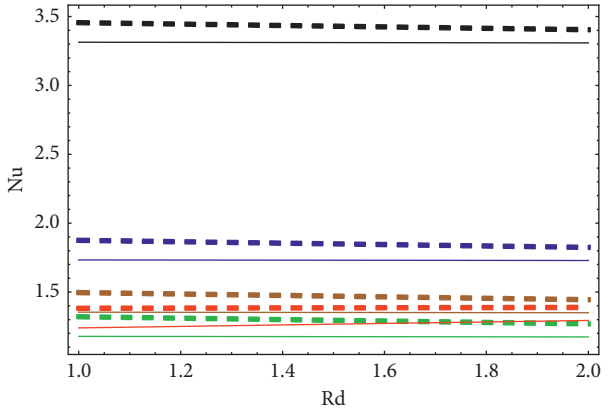

Figure 6: Nu for values of R and M, $A = 0.5$, Ec = 0.3, and $\phi = 0.2$. Blue: column. Green: sphere. Red: hexahedron. Brown: tetrahedron. Black: lamina. $R = 0.5$ solid line; $R = 1.0$ dash line.

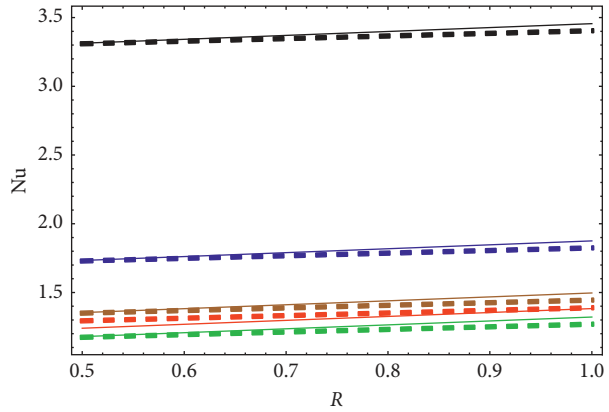

Figure 7: Nu for values of Rd and M, $A = 0.5$, Ec $= 0.3$, and $\phi = 0.2$. Blue: column. Green: sphere. Red: hexahedron. Brown: tetrahedron. Black: lamina. Rd $= 1.0$ solid line; Rd $= 2.0$ dash line.

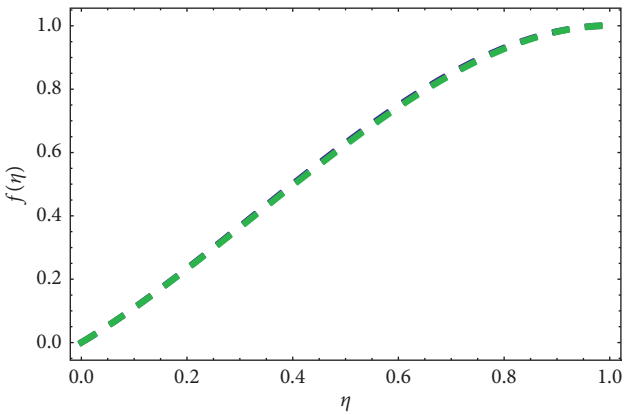

Figure 10: $f'(\eta)$ for values of M and $R = 0.3$, $A = 1.0$, and $\phi = 0.2$. Blue: $M = 0.5$. Green: $M = 4.0$.

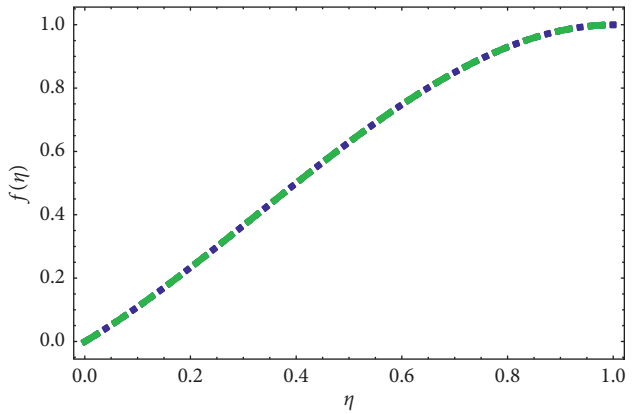

Figure 8: $f'(\eta)$ for values of ϕ and $R = 0.3$, $M = 0.5$, and$A = 1.0$. Blue: $\phi = 0.1$. Green: $\phi = 0.2$.

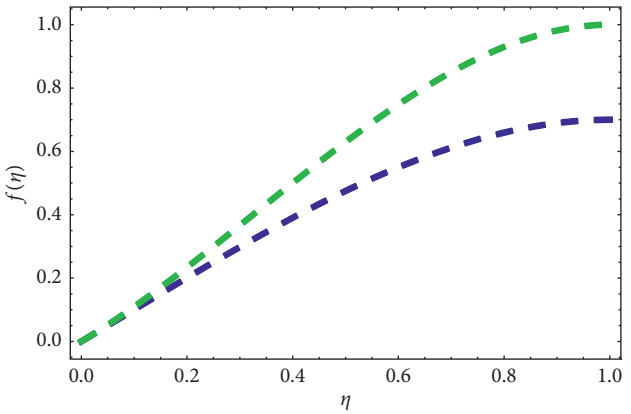

Figure 11: $f'(\eta)$ for values of A and $R = 0.3$, $M = 0.5$, and $\phi = 0.2$. Blue: $A = 0.5$. Green: $A = 1.0$.

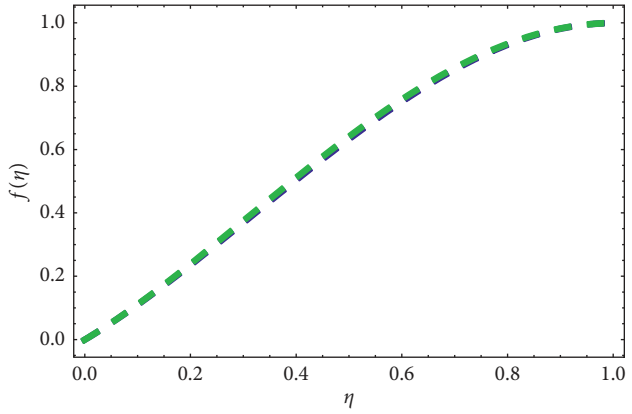

Figure 9: $f'(\eta)$ for values of R and $M = 0.5$, $A = 1.0$, and $\phi = 0.2$. Blue: $R = 0.5$. Green: $R = 1.0$.

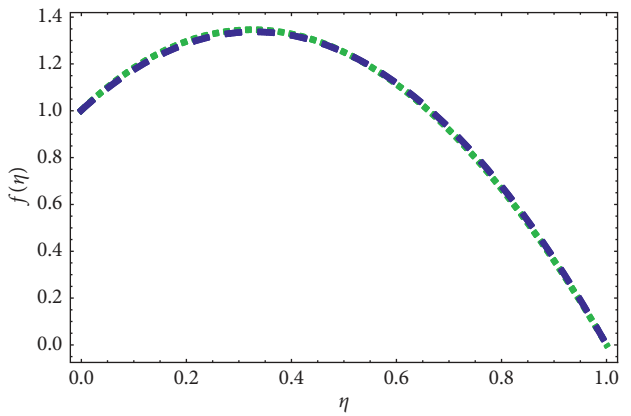

Figure 12: $f'(\eta)$ for values of M and $R = 0.3$, $A = 1.0$, and $\phi = 0.2$. Blue: $\phi = 0.1$. Green: $\phi = 0.2$.

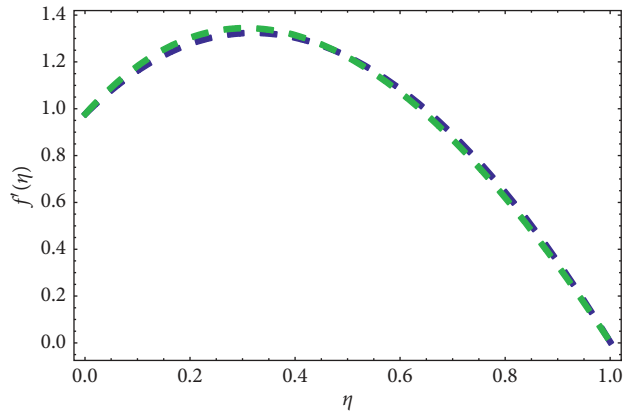

FIGURE 13: $f'(\eta)$ for values of R and $M = 0.5$, $A = 1.0$, and $\phi = 0.2$. Blue: $R = 0.5$. Green: $R = 1.0$.

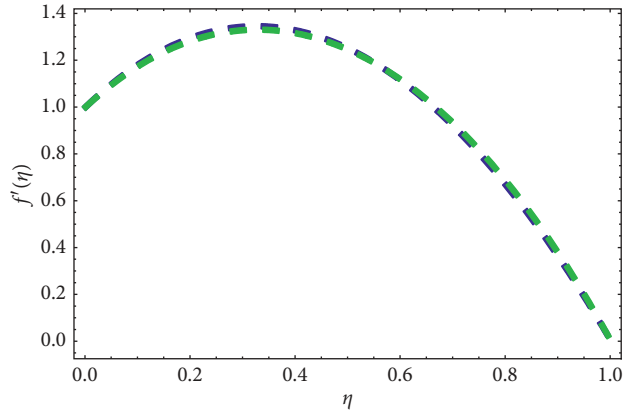

FIGURE 14: $f'(\eta)$ for values of M and $R = 0.3$, $A = 1.0$, and $\phi = 0.2$. Blue: $M = 0.5$. Green: $M = 4.0$.

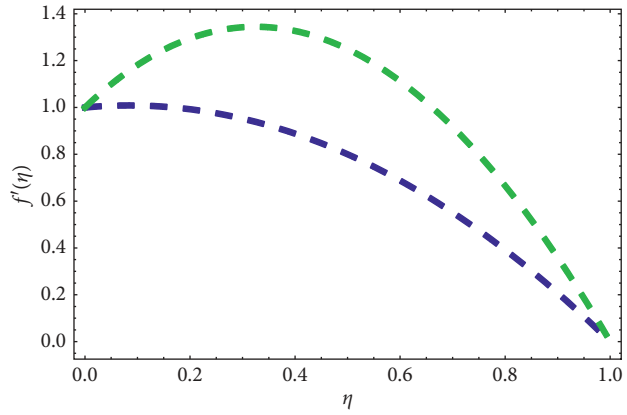

FIGURE 15: $f'(\eta)$ for values of A and $R = 0.3$, $M = 0.5$, and $\phi = 0.2$. Blue: $A = 0.5$. Green: $A = 1.0$.

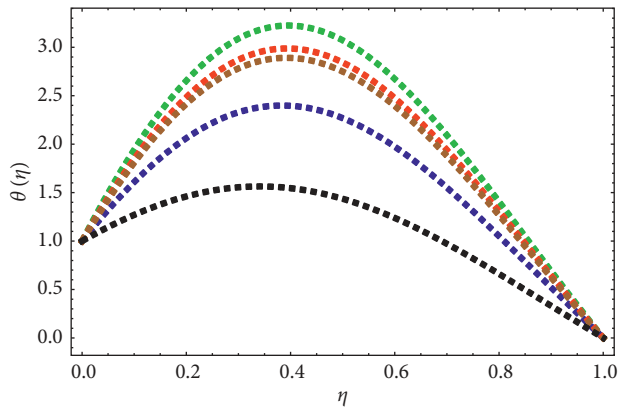

FIGURE 16: $\theta(\eta)$ for effect of the nanoparticles shapes and $R = 0.3$, Rd, $M = 0.5$, Ec $= 0.7$, $A = 1.0$, and $\phi = 0.2$. Blue: column. Green: sphere. Red: hexahedron. Brown: tetrahedron. Black: lamina.

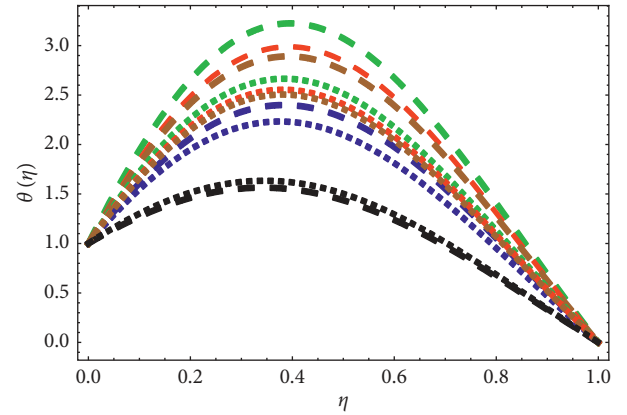

FIGURE 17: $\theta(\eta)$ for values of ϕ and Ec $= 0.7$, Rd, $M = 0.5$, $R = 0.3$, and $A = 1.0$. Blue: column. Green: sphere. Red: hexahedron. Brown: tetrahedron. Black: lamina. $\phi = 0.1$ dot line; $\phi = 0.2$ dash line.

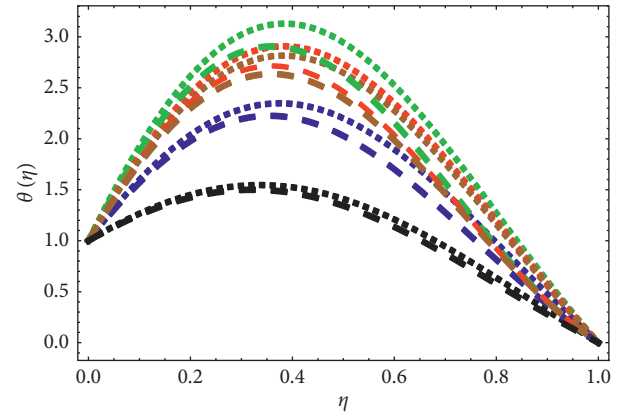

FIGURE 18: $\theta(\eta)$ for values of R and Ec $= 0.7$, Rd, $M = 0.5$, $A = 1.0$, and $\phi = 0.2$. Blue: column. Green: sphere. Red: hexahedron. Brown: tetrahedron. Black: lamina. $R = 0.5$ dot line; $R = 1.0$ dash line.

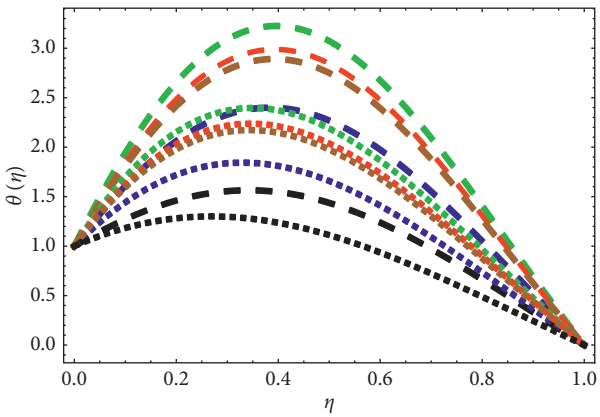

Figure 19: $\theta(\eta)$ for values of M and $R = 0.3$, Rd $= 0.5$, Ec $= 0.7$, $A = 1.0$, and $\phi = 0.2$. Blue: column. Green: sphere. Red: hexahedron. Brown: tetrahedron. Black: lamina. $M = 1.0$ dot line; $M = 3.0$ dash line.

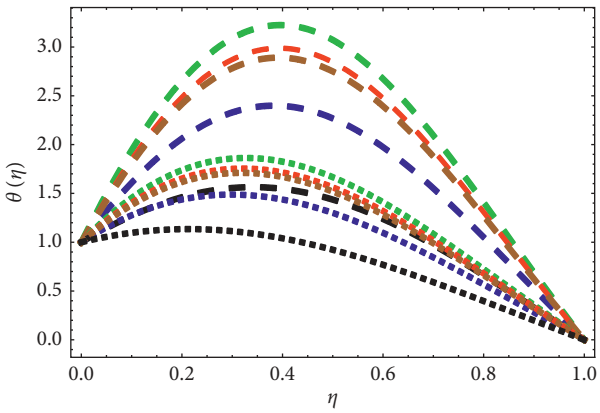

Figure 20: $\theta(\eta)$ for values of A and $R = 0.3$, Rd, $M = 0.5$, Ec $= 0.7$, and $\phi = 0.2$. Blue: column. Green: sphere. Red: hexahedron. Brown: tetrahedron. Black: lamina. $A = 0.7$ dot line; $A = 1.0$ dash line.

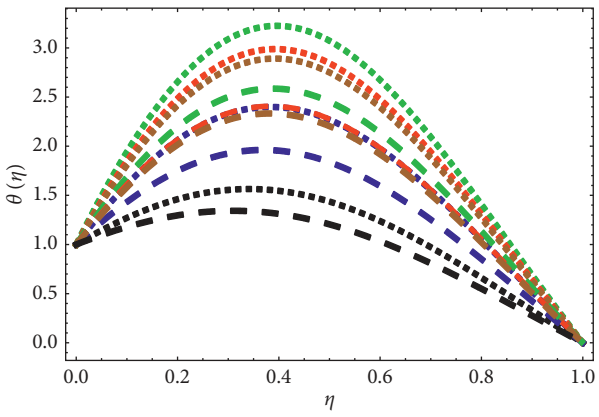

Figure 21: $\theta(\eta)$ for values of Rd and Ec $= 0.7$, $R = 0.3$, $M = 0.5$, $A = 1.0$, and $\phi = 0.2$. Blue: column. Green: sphere. Red: hexahedron. Brown: tetrahedron. Black: lamina. Rd $= 0.5$ dot line; Rd $= 1.0$ dash line.

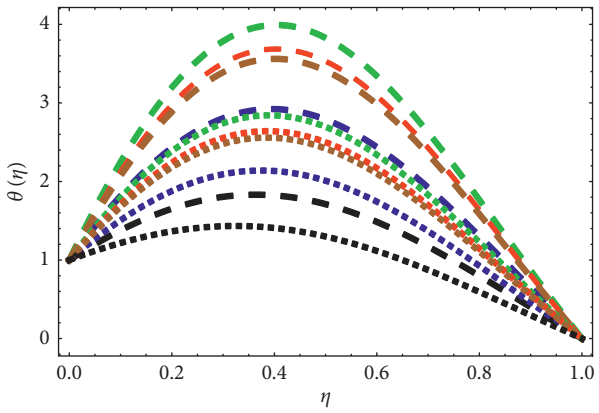

Figure 22: $\theta(\eta)$ for values of Ec and $R = 0.3$, Rd, $M = 0.5$, $A = 1.0$, and $\phi = 0.2$. Blue: column. Green: sphere. Red: hexahedron. Brown: tetrahedron. Black: lamina. Ec $= 0.6$ dot line; Ec $= 0.9$ dash line.

that the effect of sphere shape nanoparticles is more significant than other shapes of nanoparticles under the influence of R. Figure 19 describes the impact of M on thermal boundary layer thickness. From Figure 19, it is noted that the temperature increases with the increase of M. The reason is that M tends to increase a dragging force which produces heat in temperature profile. Figure 19 depicts that the sphere shape nanoparticles in Au-water play a leading role in the temperature profile. Figure 20 shows that the temperature profile increases with A; physically, the heated nanofluid is pushed towards the wall, where the buoyancy forces can intensify the viscosity. That is why it decreases the wall shear stress. Figure 21 shows the effect of Rd on temperature profile; from this figure, it is illustrated that the Rd has an inverse relation with temperature profile. Due to this, the greater value of Rd corresponds to an increase in the dominance of conduction over radiation and hence reduction in the buoyancy force and the thermal boundary layer thickness. Under the effect of Rd, sphere shape nanoparticles have an important role in temperature distribution. Figure 22 displays that the squeezed nanofluid flow temperature increases with the increase of the Ec; the reason is that the frictional heat is deposited in squeezed nanofluid; however, thermal boundary layer thickness of sphere shape nanoparticles seems to be more animated in squeezed nanofluid by Ec effect.

5. Conclusion

In the present paper, the effect of gold (Au) nanoparticles on squeezing nanofluid flow has been thoroughly examined. The analytical solution was obtained by using homotopy analysis method (HAM) for a range of pertinent parameters such as shape factor, solid volume fraction, thermal radiation, Reynolds number, magnetic field, suction parameter, and Eckert number. The effects of various parameters have been illustrated through graphs. The Pr keeps fixed at 6.2. In the view of results and discussions, the following deductions have arrived:

(i) The nanoparticles of sphere shape show a remarkable role in the disturbance of temperature profiles

(ii) The nanoparticles of tetrahedron shape show a moderate role in the disturbance of temperature profiles

(iii) The nanoparticles of lamina shape play a lower role in the disturbance of temperature profiles

(iv) The nanoparticles of lamina shape play a principal role in the heat transfer rate

(v) The nanoparticles of tetrahedron shape show a moderate role in the heat transfer rate

(vi) The nanoparticles of tetrahedron shape show a lower role in the heat transfer rate

(vii) Performances of lamina and sphere shapes nanoparticles in the forms of disturbance on temperature profiles and the heat transfer are opposite to each other

(viii) Performances of hexahedron and tetrahedron shapes nanoparticles in forms of the disturbance temperature profiles and the heat transfer are opposite to each other

Abbreviations

PDEs: Partial differential equations
ODEs: Ordinary differential equations
RNA: Ribonucleic acid
DNA: Deoxyribonucleic acid
MHD: Magnetohydrodynamic
HPM: Homotopy perturbation method
HAM: Homotopy analysis method.

Data Availability

No data were used to support this study.

Conflicts of Interest

The authors declare no conflicts of interest.

Authors' Contributions

Umair Rashid, Azhar Iqbal, and Mohd. Junaid Siddiqui contributed to conceptualization; Umair Rashid, Thabet Abdeljawad, and Azhar Iqbal contributed to methodology; Umair Rashid, Haiyi Liang, Azhar Iqbal, and Muhammad Abbas contributed to software; Haiyi Liang, Umair Rashid, Thabet Abdeljawad, Azhar Iqbal, Mohd. Junaid Siddiqui, and Muhammad Abbas contributed to validation; Haiyi Liang, Umair Rashid, Thabet Abdeljawad, Azhar Iqbal, Mohd. Junaid Siddiqui, and Muhammad Abbas contributed to formal analysis; Haiyi Liang, Umair Rashid, Thabet Abdeljawad, Azhar Iqbal, Mohd. Junaid Siddiqui, and Muhammad Abbas contributed to investigation; Thabet Abdeljawad and Muhammad Abbas contributed to resources; Umair Rashid, Azhar Iqbal, and Muhammad Abbas are responsible for writing and original draft preparation; Haiyi Liang, Umair Rashid, Azhar Iqbal, and Muhammad Abbas are responsible for writing, review, and editing of the paper; Azhar Iqbal and Muhammad Abbas contributed to visualization; Haiyi Liang, Thabet Abdeljawad, and Muhammad Abbas contributed to supervision; Thabet Abdeljawad and Muhammad Abbas contributed to funding acquisition. All authors have read and agreed to the published version of the manuscript.

Acknowledgments

The authors thank Dr. Muhammad Kashif Iqbal, GC University, Faisalabad, Pakistan, for his assistance in proofreading the manuscript. The authors would like to acknowledge Prince Sultan University for funding this work through the research group Nonlinear Analysis Methods in Applied Mathematics (NAMAM) (Group no. RG-DES-2017-01-17).

References

[1] M. Das, K. H. Shim, S. S. A. An, and D. K. Yi, "Review on gold nanoparticles and their applications," *Toxicology and Environmental Health Sciences*, vol. 3, no. 4, pp. 193–205, 2011.

[2] S. Muhammad, S. Shah, G. Ali, M. Ishaq, S. Hussain, and H. Ullah, "Squeezing nanofluid flow between two parallel plates under the influence of MHD and thermal radiation," *Asian Research Journal of Mathematics*, vol. 10, no. 1, pp. 1–20, 2018.

[3] T. Hayat, T. Abbas, M. Ayub, T. Muhammad, and A. Alsaedi, "On squeezed flow of jeffrey nanofluid between two parallel disks," *Applied Sciences*, vol. 6, pp. 1–15, 2016.

[4] A. Dib, A. Haiahem, and B. Bou-said, "Approximate analytical solution of squeezing unsteady nanofluid flow," *Powder Technology*, vol. 269, pp. 193–199, 2015.

[5] H. M. Duwairi, B. Tashtoush, and R. A. Damseh, "On heat transfer effects of a viscous fluid squeezed and extruded between two parallel plates," *Heat and Mass Transfer*, vol. 41, pp. 112–117, 2004.

[6] G. Domairry and M. Hatami, "Squeezing Cu-water nanofluid flow analysis between parallel plates by DTM-Padé method," *Journal of Molecular Liquids*, vol. 193, pp. 37–44, 2014.

[7] M. Sheikholeslami and D. D. Ganji, "Heat transfer of Cu-water nanofluid flow between parallel plates," *Powder Technology*, vol. 235, pp. 873–879, 2013.

[8] S. I. Khan, U. Khan, N. Ahmed, and S. T. Mohyud-Din, "Thermal radiation effects on squeezing flow casson fluid between parallel disks," *Communications in Numerical Analysis*, vol. 2016, no. 2, pp. 92–107, 2016.

[9] M. Sheikholeslami, M. Hatami, and D. D. Ganji, "Nanofluid flow and heat transfer in a rotating system in the presence of a magnetic field," *Journal of Molecular Liquids*, vol. 190, pp. 112–120, 2014.

[10] A. K. Gupta and S. Saha Ray, "Numerical treatment for investigation of squeezing unsteady nanofluid flow between two parallel plates," *Powder Technology*, vol. 279, pp. 282–289, 2015.

[11] M. Mahmoodi and S. Kandelousi, "Kerosene–alumina nanofluid flow and heat transfer for cooling application," *Journal of Central South University*, vol. 23, no. 4, pp. 983–990, 2016.

[12] S. Liao, "An optimal homotopy-analysis approach for strongly nonlinear differential equations," *Communications in Nonlinear Science and Numerical Simulation*, vol. 15, no. 8, pp. 2003–2016, 2010.

[13] S. Liao, "An analytic solution of unsteady boundary-layer flows caused by an impulsively stretching plate," *Communications in Nonlinear Science and Numerical Simulation*, vol. 11, no. 3, pp. 326–339, 2006.

[14] S. Liao, "On the homotopy analysis method for nonlinear problems," *Applied Mathematics and Computation*, vol. 147, no. 2, pp. 499–513, 2004.

[15] S.-J. Liao, "On the analytic solution of magnetohydrodynamic flows of non-Newtonian fluids over a stretching sheet," *Journal of Fluid Mechanics*, vol. 488, pp. 189–212, 2003.

[16] S.-J. Liao, "An explicit, totally analytic approximate solution for Blasius' viscous flow problems," *International Journal of Non-linear Mechanics*, vol. 34, no. 4, pp. 759–778, 1999.

[17] M. M. Rashidi, A. M. Siddiqui, and M. Asadi, "Application of homotopy analysis method to the unsteady squeezing flow of a second-grade fluid between circular plates," *Mathematical Problems in Engineering*, vol. 2010, Article ID 706840, 18 pages, 2010.

[18] M. M. Rashidi and S. A. Mohimanian Pour, "Analytic approximate solutions for unsteady boundary-layer flow and heat transfer due to a stretching sheet by homotopy analysis method," *Nonlinear Analysis: Modelling and Control*, vol. 15, no. 1, pp. 83–95, 2010.

[19] S. Abbasbandy, "Homotopy analysis method for heat radiation equations," *International Communications in Heat and Mass Transfer*, vol. 34, no. 3, pp. 380–387, 2007.

[20] S. Abbasbandy and A. Shirzadi, "A new application of the homotopy analysis method: solving the Sturm-Liouville problems," *Communications in Nonlinear Science and Numerical Simulation*, vol. 16, no. 1, pp. 112–126, 2011.

[21] S. Hussain, S. Muhammad, G. Ali et al., "A bioconvection model for squeezing flow between parallel plates containing gyrotactic microorganisms with impact of thermal radiation and heat generation/absorption," *Journal of Advances in Mathematics and Computer Science*, vol. 27, no. 4, pp. 1–22, 2018.

[22] O. Manca, Y. Jaluria, G. Lauriat, K. Vafai, and L. Wang, "Heat transfer in nanofluids 2013," *Advances in Mechanical Engineering*, vol. 2014, Article ID 832415, 2 pages, 2014.

[23] W. Yu and H. Xie, "A review on nanofluids: preparation, stability mechanisms, and applications," *Journal of Nanomaterials*, vol. 2012, Article ID 435873, 17 pages, 2012.

[24] Y. Xuan and Q. Li, "Heat transfer enhancement of nanofluids," *International Journal of Heat and Fluid Flow*, vol. 21, no. 1, pp. 58–64, 2000.

[25] B. Kristiawan, B. Santoso, A. T. Wijayanta, M. Aziz, and T. Miyazaki, "Heat transfer enhancement of TiO_2/water nanofluid at laminar and turbulent flows: a numerical approach for evaluating the effect of nanoparticle loadings," *Energies*, vol. 11, no. 6, Article ID 1584, 2018.

[26] M. Turkyilmazoglu and I. Pop, "Heat and mass transfer of unsteady natural convection flow of some nanofluids past a vertical infinite flat plate with radiation effect," *International Journal of Heat and Mass Transfer*, vol. 59, pp. 167–171, 2013.

[27] L. Qiang and X. Yimin, "Convective heat transfer and flow characteristics of Cu-water nanofluid," *Science in China, Series E: Technological Sciences*, vol. 45, no. 4, pp. 408–416, 2002.

[28] N. S. Elgazery, "Nanofluids flow over a permeable unsteady stretching surface with non-uniform heat source/sink in the presence of inclined magnetic field," *Journal of the Egyptian Mathematical Society*, vol. 27, no. 1, pp. 1–26, 2019.

[29] U. Rea, T. McKrell, L.-w. Hu, J. Buongiorno, and J. Buongiorno, "Laminar convective heat transfer and viscous pressure loss of alumina-water and zirconia-water nanofluids," *International Journal of Heat and Mass Transfer*, vol. 52, no. 7-8, pp. 2042–2048, 2009.

[30] B. H. Salman, H. A. Mohammed, and A. S. Kherbeet, "Heat transfer enhancement of nanofluids flow in microtube with constant heat flux," *International Communications in Heat and Mass Transfer*, vol. 39, no. 8, pp. 1195–1204, 2012.

[31] M. Sheikholeslami, R. Ellahi, and C. Fetecau, "CuO–water nanofluid magnetohydrodynamic natural convection inside a sinusoidal annulus in presence of melting heat transfer," *Mathematical Problems in Engineering*, vol. 2017, Article ID 5830279, 9 pages, 2017.

[32] S. Manikandan and K. S. Rajan, "New hybrid nanofluid containing encapsulated paraffin wax and sand nanoparticles in propylene glycol-water mixture: potential heat transfer fluid for energy management," *Energy Conversion and Management*, vol. 137, pp. 74–85, 2017.

[33] M. Hassan, M. Marin, R. Ellahi, and S. Z. Alamri, "Exploration of convective heat transfer and flow characteristics synthesis by Cu-Ag/water hybrid-nanofluids," *Heat Transfer Research*, vol. 49, no. 18, pp. 1837–1848, 2018.

[34] M. M. Bhatti, R. Ellahi, A. Zeeshan, M. Marin, and N. Ijaz, "Numerical study of heat transfer and Hall current impact on peristaltic propulsion of particle-fluid suspension with compliant wall properties," *Modern Physics Letters B*, vol. 33, no. 35, Article ID 1950439, 2019.

[35] G. Palani and I. A. Abbas, "Free convection MHD flow with thermal radiation from an impulsively-started vertical plate," *Nonlinear Analysis: Modelling and Control*, vol. 14, no. 1, pp. 73–84, 2009.

[36] K. Sharma and M. Marin, "Reflection and transmission of waves from imperfect boundary between two heat conducting micropolar thermoelastic solids," *Analele Universitatii "Ovidius" Constanta—Seria Matematica*, vol. 22, no. 2, pp. 151–176, 2014.

[37] S. M. Atif, S. Hussain, and M. Sangheer, "Effect of viscous dissipation and Joule heating on MHD radiative tangent hyperbolic nanofluid with convective and slip conditions," *Journal of the Brazilian Society of Mechanical Sciences and Engineering*, vol. 41, no. 4, p. 189, 2019.

[38] S. M. Atif, S. Hussain, and M. Sagheer, "Heat and mass transfer analysis of time-dependent tangent hyperbolic nanofluid flow past a wedge," *Physics Letters A*, vol. 383, no. 11, pp. 1187–1198, 2019.

[39] U. Rashid and A. Ibrahim, "Impacts of nanoparticle shape on Al_2O_3-water nanofluid flow and heat transfer over a nonlinear radically stretching sheet," *Advances in Nanoparticles*, vol. 9, no. 1, pp. 23–39, 2020.

[40] S. Aman, I. Khan, Z. Ismail, and M. Z. Salleh, "Impacts of gold nanoparticles on MHD mixed convection Poiseuille flow of nanofluid passing through a porous medium in the presence of thermal radiation, thermal diffusion and chemical reaction," *Neural Computing and Applications*, vol. 30, no. 3, pp. 789–797, 2018.

[41] R. Kandasamy, N. A. bt Adnan, and R. Mohammad, "Nanoparticle shape effects on squeezed MHD flow of water based Cu, Al_2O_3 and SWCNTs over a porous sensor surface," *Alexandria Engineering Journal*, vol. 57, no. 3, pp. 1433–1445, 2018.

[42] M. Mahmoodi and S. Kandelousi, "Semi-analytical investigation of kerosene-alumina nanofluid between two parallel plates," *Journal of Aerospace Engineering*, vol. 29, no. 4, Article ID 04016001, 2016.

[43] N. A. Adnan, R. Kandasamy, and R. Mohammad, "Nanoparticle shape and thermal radiation on marangoni water,

ethylene glycol and engine oil based Cu, Al_2O_3 and SWCNTs," *Journal of Material Sciences & Engineering*, vol. 6, no. 4, 2017.

[44] Y. Lin, B. Li, L. Zheng, and G. Chen, "Particle shape and radiation effects on Marangoni boundary layer flow and heat transfer of copper-water nanofluid driven by an exponential temperature," *Powder Technology*, vol. 301, pp. 379–386, 2016.